

Iron chelator deferoxamine alters iron-regulatory genes and proteins and suppresses osteoblast phenotype in fetal rat calvaria cells

By: Jonathan G. Messer, Paula T. Cooney, [Deborah E. Kipp](#)

Messer, J.G., Cooney, P.T., Kipp, D.E. Iron chelator deferoxamine alters iron-regulatory genes and proteins and suppresses osteoblast phenotype in fetal rat calvaria cells. *Bone* 46(5): 1408-1415, 2010.

Made available courtesy of Elsevier: <http://www.dx.doi.org/10.1016/j.bone.2010.01.376>

***© Elsevier. Reprinted with permission. No further reproduction is authorized without written permission from Elsevier. This version of the document is not the version of record. Figures and/or pictures may be missing from this format of the document. ***

This is the author's version of a work that was accepted for publication in *Bone*. Changes resulting from the publishing process, such as peer review, editing, corrections, structural formatting, and other quality control mechanisms may not be reflected in this document. Changes may have been made to this work since it was submitted for publication. A definitive version was subsequently published in *Bone*, Vol.46, Issue 5, (2010) DOI: 10.1016/j.bone.2010.01.376

Abstract:

There are few studies describing the extent to which low iron status affects osteoblastogenesis, despite evidence that iron deficiency produces adverse effects on bone density. The purpose of this study was to evaluate alterations in intracellular iron status by measuring iron-regulated gene and protein expression and to describe development of osteoblast phenotype in primary cells treated with iron chelator deferoxamine (DFOM) during differentiation. Using the well-described fetal rat calvaria model, cells were incubated with 0–8 μM DFOM throughout differentiation (confluence to day (D) 21), or only during early differentiation (confluence to D13–15) or late differentiation (D13–15 to D21). Changes in intracellular iron status were determined by measuring alterations in gene and protein expression of transferrin receptor and ferritin light chain and heavy chain. Development of osteoblast phenotype was monitored by measuring expression of genes that are known to be up-regulated during differentiation, analyzing the percentage of mineralized surface area, and counting the number of multi-layered bone nodules at the end of culture. Results indicate that treatment throughout differentiation with 8 μM DFOM alters iron-regulated genes and proteins by mid-differentiation (D13–15) in a pattern consistent with iron deficiency with concomitant down-regulation of osteoblast phenotype genes, especially osteocalcin. Additionally, alkaline phosphatase staining was lower and there was about 70% less mineralized surface area ($p < 0.05$) by D21 in wells treated throughout differentiation with 8 μM DFOM compared to control. Down-regulation of osteocalcin and alkaline phosphatase mRNA ($p < 0.05$) and suppressed mineralization ($p < 0.05$) was also evident at D21 in cells treated only

during early differentiation. In contrast, treatment during late differentiation did not alter osteoblastic outcomes by D21. In conclusion, it appears that iron is required for normal osteoblast phenotype development, and that early rather than late differentiation events may be more sensitive to iron availability.

Keywords: Transferrin receptor | Ferritin | Iron deficiency | Osteocalcin | Bone nodules

Article:

Introduction

Iron deficiency is typically attributed to inadequate dietary intake, blood loss, or chronic inflammation [1] and is estimated to affect more than 2 billion people worldwide, particularly women and children [2]. Due to iron's indispensable role in numerous biochemical reactions, low body iron stores result in deleterious effects on the function of a number of biological systems [3].

Evidence from studies conducted in both humans and rats suggests that iron is necessary for balanced bone metabolism. Dietary iron intake appears to be associated with a protective effect on bone density in post-menopausal women [4], [5] and [6], while moderate to severe dietary iron deficiency in rats results in altered bone morphology and microarchitecture, decreased density and strength in femurs and vertebrae, and increased urinary bone turnover markers [7], [8], [9] and [10]. Research specifically examining the effects of iron deficiency on bone formation *in vitro* is limited. Naves Díaz et al [11] reported higher activity of alkaline phosphatase, a non-specific marker of osteoblastogenic potential [12], compared to control in MG-63 osteosarcoma cells after 48 and 96 h of treatment with deferoxamine (DFOM) or deferiprone. Conversely, Parelman et al [13] reported lower amounts of Alizarin red staining and increased transferrin receptor (TrfR) protein expression in hFOB 1.19 cells compared to control after acute exposure (48-96 h) to DFOM. There have been no studies specifically examining the influence of low iron availability on osteoblast maturation and function.

Studies conducted in differentiating primary cells, rather than immortal cell lines, may be best suited to address questions related to iron deficiency induced changes in bone formation, since primary cells are believed to express osteoblast phenotype genes and produce extracellular matrix most similar to that of osteoblasts *in vivo* [14] and [15]. Therefore, in the present study, experiments were designed to generate low intracellular iron levels in primary cell cultures isolated from fetal rat calvaria, a well defined model of osteoblast differentiation which exhibits temporal regulation of osteoblast phenotype gene markers and culminates in nodules similar to woven bone [15]. Iron status was altered by treatment with DFOM, a membrane-permeable iron chelator shown to prevent iron uptake [16] and chelate iron from the intracellular iron pool [17]. Using this experimental model the effect of DFOM on iron-regulated genes and proteins and the extent to which low iron availability affects osteoblast phenotypic development and function could be evaluated.

Materials and methods

Animal care

Female Sprague-Dawley rats were obtained on D13 of pregnancy (Harlan, SD, Raleigh, NC). Rats were housed at 19–20 ° C with a 12 h light-dark cycle and had free access to Harlan Teklad 7002 6% mouse/rat diet and water. At D21 of pregnancy, dams were euthanized by CO₂ overdose, pups were collected, and calvaria were aseptically removed [18]. All procedures were approved by the University of North Carolina at Greensboro Animal Care and Use Committee.

Calvaria cultures

Cells were enzymatically released from the calvaria in five sequential collagenase digestions as previously described [18]. Cells from the last four incubations were plated in separate T-75 flasks and incubated 24 h in α -MEM (Invitrogen) containing 15% heat-inactivated fetal bovine serum (FBS) (Invitrogen) and 10% antibiotics. Antibiotics consisted of 1 mg/ml penicillin (Sigma), 0.5 mg/ml gentamicin (Invitrogen), and 2.5 μ g/ml fungizone (Invitrogen). Cells from each flask were trypsinized, pooled, and seeded at 3000 cells/cm² in 6 well plates. Cells were incubated up to 21 days at 37 ° C with 5% CO₂ in complete media containing α -MEM, 10% FBS, 10% antibiotics, 25 μ g/ml ascorbic acid, 10 mM sodium β -glycerolphosphate, and 10⁻⁸ M dexamethasone. Fresh media was provided every 2-3 days. DFOM (Sigma) was diluted to final concentrations in fresh media and delivered during media changes beginning at confluence (~ D8) and either throughout the 2-week differentiation period, or only during the first or second week. Deionized water was the vehicle control (0 μ M).

Preliminary study

A preliminary study was performed to establish the dose response relationship of DFOM and osteogenic outcomes in fetal rat calvaria cultures. Doses ranging from 0 to 32 μ M DFOM were administered in fresh media at media changes throughout the differentiation period (confluence to D21). Samples were collected on D21 and percent mineralized surface area was analyzed (see below) along with gene expression of osteoblast phenotype markers using real-time PCR (see below).

Real-time RT-PCR

Cells were collected by scraping in 1 ml of TRIZOL (Invitrogen). Three separate wells were pooled per sample. RNA was extracted using procedures specified by the manufacturer and purity and concentrations were determined using NanoDrop Spectrophotometer ND-1000 (NanoDrop Technologies, Inc.). Two micrograms of RNA was reverse transcribed using High Capacity cDNA Reverse Transcription Kit (Applied Biosystems) in the presence of 1 U/ μ l RNasin Ribonuclease Inhibitor (Promega).

Fifty nanograms of cDNA was amplified using Taqman Fast Universal Mastermix and Taqman Gene Expression assays (Applied Biosystems) for rat. Osteoblast phenotype markers included alkaline phosphatase (ALP), bone sialoprotein (BSP), and osteocalcin (OCN). Runx2, a key transcription factor involved in osteoblast differentiation, was also analyzed. Iron genes included TrfR, ferritin heavy chain (FerH), and ferritin light chain (FerL). Ribosomal protein, L32, was used as the endogenous control. Relative gene expression was quantified using the delta-delta Ct method. Genomic DNA contaminants contributed to less than 1% of the amplification signal in assays that used primers that were not designed around exon boundaries (L32, FerH, and FerL), and were therefore considered negligible.

Western blotting

Cells from 3 separate wells were lysed and pooled in cold RIPA buffer, containing 10 mM sodium fluoride, 20 mM β -glycerolphosphate, 0.1 mM sodium orthovanadate, and either protease inhibitor cocktail (Calbiochem) or 0.5 mM PMSF and 0.1 μ g/ μ l aprotinin. Lysates were stored at -80° C until further analysis. Lysates were thawed and sonicated on ice, and centrifuged at $16,000 \times g$ for 20 min. Supernatants were removed and protein concentrations were determined with BCA assay by manufacturer's instructions (Pierce).

Twenty micrograms of proteins per well was resolved on NuPage 4-12% bis-tris gels (Invitrogen). Proteins were transferred onto polyvinylidene difluoride membranes (Immobilon) and blocked in 5% (w/v) milk dissolved in Tris-buffered saline with 0.05% (v/v) Tween-20 (TBS-T) (Sigma). Membranes were then incubated with primary antibodies overnight at 4° C, washed in TBS-T, and incubated with secondary antibodies for 30 min at room temperature. Primary antibodies were diluted in 5% (w/v) bovine serum albumin (Sigma) in TBS-T and included mouse anti- β -actin (Sigma), mouse anti-transferrin receptor (Zymed), and rabbit anti-ferritin (Abcam), which recognize both heavy and light subunits. HRP-conjugated secondary antibodies include donkey anti-mouse (Affinity BioReagents) and goat anti-rabbit (Cell Signaling). Signal was detected with Western Lightning Chemiluminescence Reagent Plus kit (PerkinElmer). Net intensity values of representative blots were determined with Kodak 1D Imaging Software (version 3.6.2) and normalized to net intensity of loading control, β -actin. Means are expressed as a percent of control.

Staining

These methods are described in detail elsewhere [19]. Briefly, cells were washed in PBS, fixed in 10% neutral formalin buffer, and rinsed with deionized water. ALP-positive cells were stained using Naphthol AS MX- PO_4 (Sigma) as substrate and Red Violet LB salt (Sigma) as coupler. Mineralized nodules were stained using the von Kossa method by incubating cells with 2.5% (w/v) silver nitrate (Fisher) solution for 30 min. Culture dishes were then rinsed in tap water and air dried overnight.

Bone nodule quantification

To assess osteoblast function, the percent mineralized surface area was analyzed semi-quantitatively with Adobe Photoshop (version 6.0). Dishes of cells stained for alkaline phosphatase and von Kossa were scanned on a flatbed scanner at a resolution of 600 dpi. Identical, rectangular images of cell layers within each well were selected. All selections were taken from the same, central-most region of the well. Percent mineralized surface area was calculated by dividing the number of pixels corresponding to mineralized foci (von Kossa staining) by the total number of pixels in each image. Means are expressed as percent of control.

Wells were also examined microscopically under a bright field illumination and mineralized and unmineralized nodules were counted (data not shown). This was used in conjunction to percent mineralized surface area analysis to verify that von Kossa staining was localized to mineralized, multi-layered nodules and to account for the presence of multi-layered, unmineralized nodules.

Statistical analysis

Data are expressed as mean \pm SEM. Statistical differences were determined using one-way analysis of variance (ANOVA) with Tukey post hoc analysis. Univariate analysis was performed to check for interactions when there were two main effects of dose and time. For real-time PCR data, there was a significant interaction between the main effects of dose and time for all genes except FerH and FerL. Therefore, ANOVA was performed within each day followed by Tukey post hoc analysis for TrfR, OCN, BSP, ALP, and Runx2. Statistics were performed using SPSS version 16.0 for Windows (SPSS Inc., Chicago, IL, USA). A *p*-value less than 0.05 was considered significant.

Results

Preliminary study to determine DFOM dose

Continuous exposure throughout differentiation to 8 μ M and 32 μ M DFOM, but not 0-4 μ M DFOM, suppressed percent mineralized surface area (Fig. 1A). Since 8 μ M DFOM was the lowest dose that produced significant suppression of mineralization and gene expression of osteoblast markers (Fig. 1B), this was the highest dose used in subsequent studies.

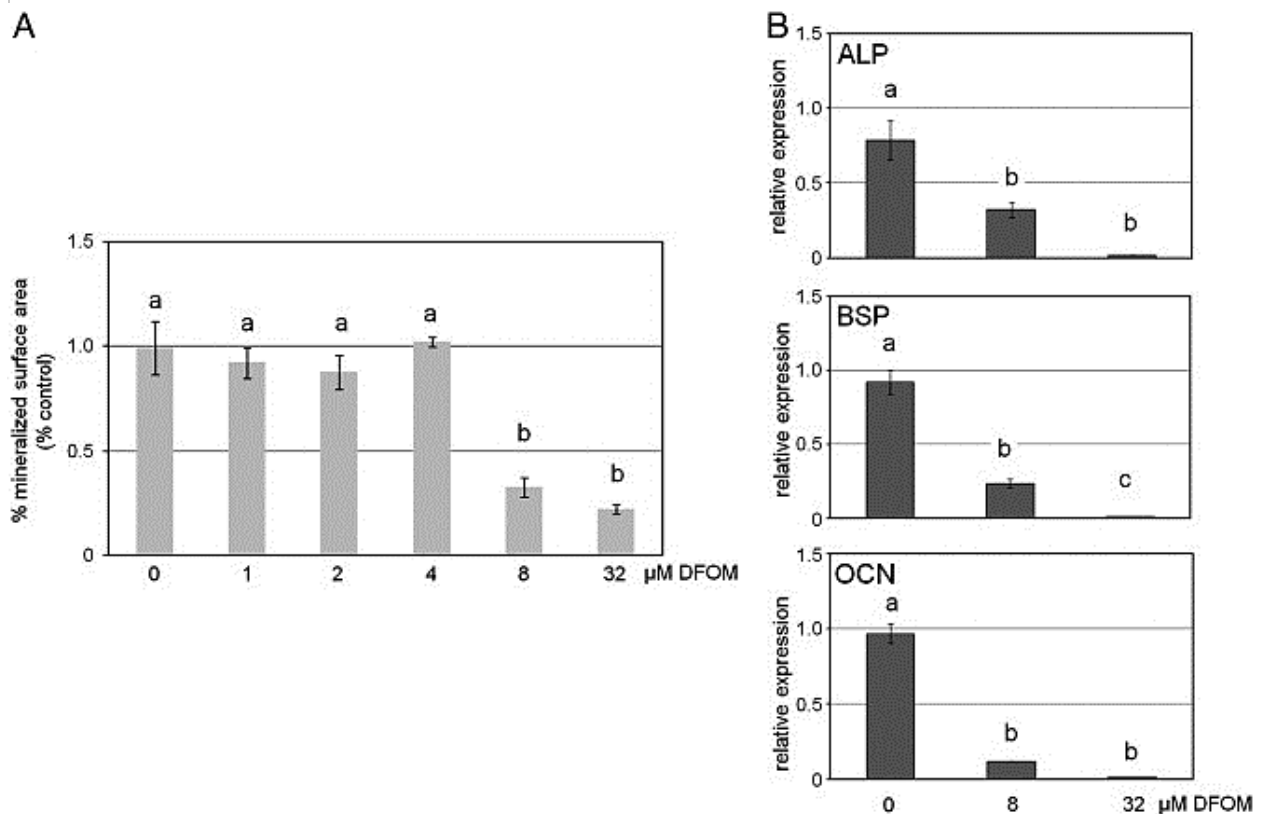


Fig. 1. Dose response relationship of chronic DFOM treatment throughout differentiation and osteoblast differentiation outcomes. (A) Average percent mineralized surface area expressed as percent control (0 μM). Data represent mean \pm SEM of 4 wells; ANOVA: $p < 0.05$. (B) Real-time PCR analysis of osteoblast phenotype genes on D21. L32 was endogenous control and 0 μM was calibrator sample. Data represent mean \pm SEM of 4 determinations; ANOVA: $p < 0.05$. Treatments that are significantly different ($p < 0.05$) as determined by Tukey post hoc analysis are assigned different letters. Treatments that are not significantly different ($p > 0.05$) are assigned the same letters.

Iron-regulated genes and proteins are altered by DFOM treatment

Real-time PCR results show that TrfR gene expression was dose-dependently up-regulated by DFOM by mid-differentiation (\sim D15) and sustained until the end of culture (D21) (Fig. 2A). TrfR proteins were congruent with gene expression, with marked and sustained up-regulation from mid-differentiation to the end of culture (Fig. 2B). Real-time PCR analysis of FerL and FerH revealed that genes were slightly up-regulated by mid-differentiation and sustained until the end of culture (Fig. 2C). Conversely, ferritin proteins were markedly down-regulated at mid-differentiation (Fig. 2D).

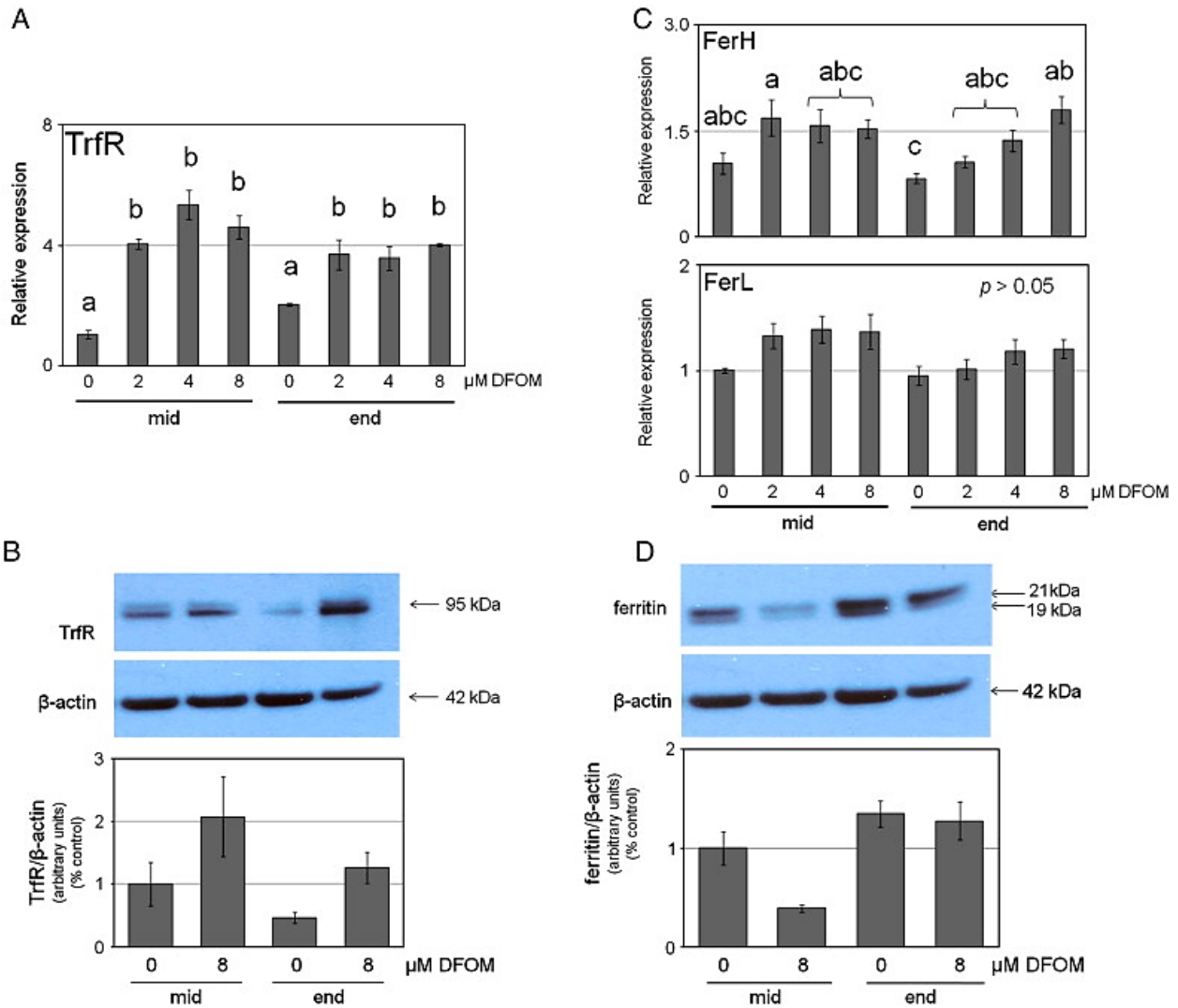


Fig. 2. Iron-regulated genes and proteins in osteoblast-like cultures isolated from fetal rat calvaria and treated with 0-8 μM DFOM throughout differentiation. Mid and end represent samples taken at midpoint (\sim D15) and end of differentiation (D21), respectively. (A) Real-time PCR amplification of TrfR with L32 as endogenous control and 0 μM mid as calibrator sample. (B) Western blots of TrfR and loading control β -actin. Semi-quantitative net intensity values normalized to β -actin and expressed as percent control (mid 0 μM). (C) Real-time PCR amplification of FerH and FerL with L32 as endogenous control and mid 0 μM as calibrator sample. (D) Western blots of ferritin subunits and β -actin. Semi-quantitative net intensity values normalized to β -actin and expressed as percent control (mid 0 μM). PCR and semi-quantitative Western blotting data represent mean \pm SEM of 4 determinations. For PCR, ANOVA: $p < 0.05$ for all genes with respect to day, except FerH and FerL. Treatments that are significantly different ($p < 0.05$) as determined by Tukey post hoc analysis are assigned different letters. Treatments that are not significantly different ($p > 0.05$) are assigned the same letters. Similar results were observed in at least 2 independent studies.

DFOM treatment suppresses mineralization and nodule development

Representative wells of cells treated with 0-8 μM DFOM and co-stained for alkaline phosphatase and von Kossa are shown in Fig. 3A. Alkaline phosphatase staining was less intense and the nodules were markedly smaller in wells treated with 8 μM DFOM than in 0-4 μM treated wells. The percent mineralized surface area was approximately 70% lower after continuous 8 μM treatment with no significant difference among 0-4 μM groups (Fig. 3B). In 8 μM DFOM treated wells the total number of nodules and the number of mineralized nodules per well were about 60% lower compared to control ($p < 0.05$, data not shown). The number of unmineralized nodules accounted for only about 20% of total nodules in control and was similar among all groups ($p > 0.05$, data not shown). Therefore, the differences in percent mineralization among treatments were primarily attributed to significantly lower numbers of mineralized nodules.

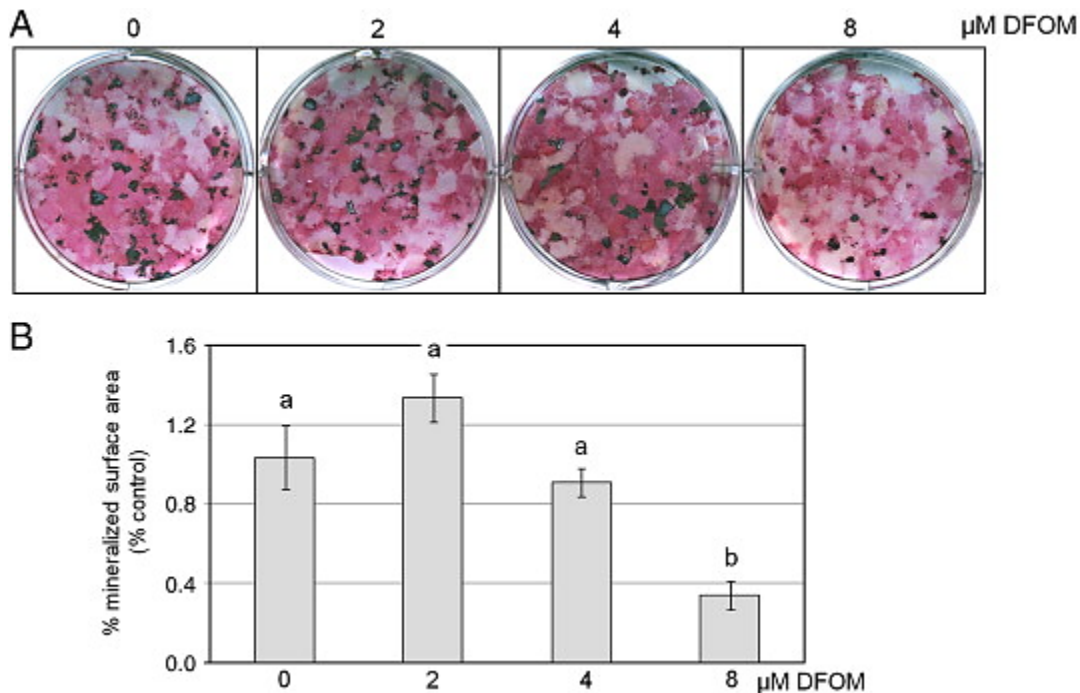


Fig. 3. Osteoblast-like colonies in cultures of fetal rat calvaria treated with 0-8 μM DFOM throughout differentiation (confluence-D21). (A) Representative wells of alkaline phosphatase-positive colonies (pink) and mineralized bone nodules (black) on D21. (B) Average percent mineralized surface area. Data represent mean \pm SEM of triplicate wells. ANOVA: $p < 0.05$; treatments that are significantly different ($p < 0.05$) as determined by Tukey post hoc analysis are assigned different letters. Treatments that are not significantly different ($p > 0.05$) are assigned the same letters. Similar results were observed in at least 2 independent studies.

Osteoblast phenotype markers are down-regulated by DFOM treatment

In fetal rat calvaria cultures, Runx2 is up-regulated the earliest, followed by ALP and BSP, and finally the most osteoblast-specific marker, OCN [15]. In the present study, gene expression in the control groups was generally consistent with typical up-regulation of osteoblast phenotype genes (Fig. 4). In contrast, all phenotype markers were dose-dependently down-regulated by mid-differentiation after treatment with 8 μ M DFOM compared to control, and suppression was sustained until end of culture (Fig. 4).

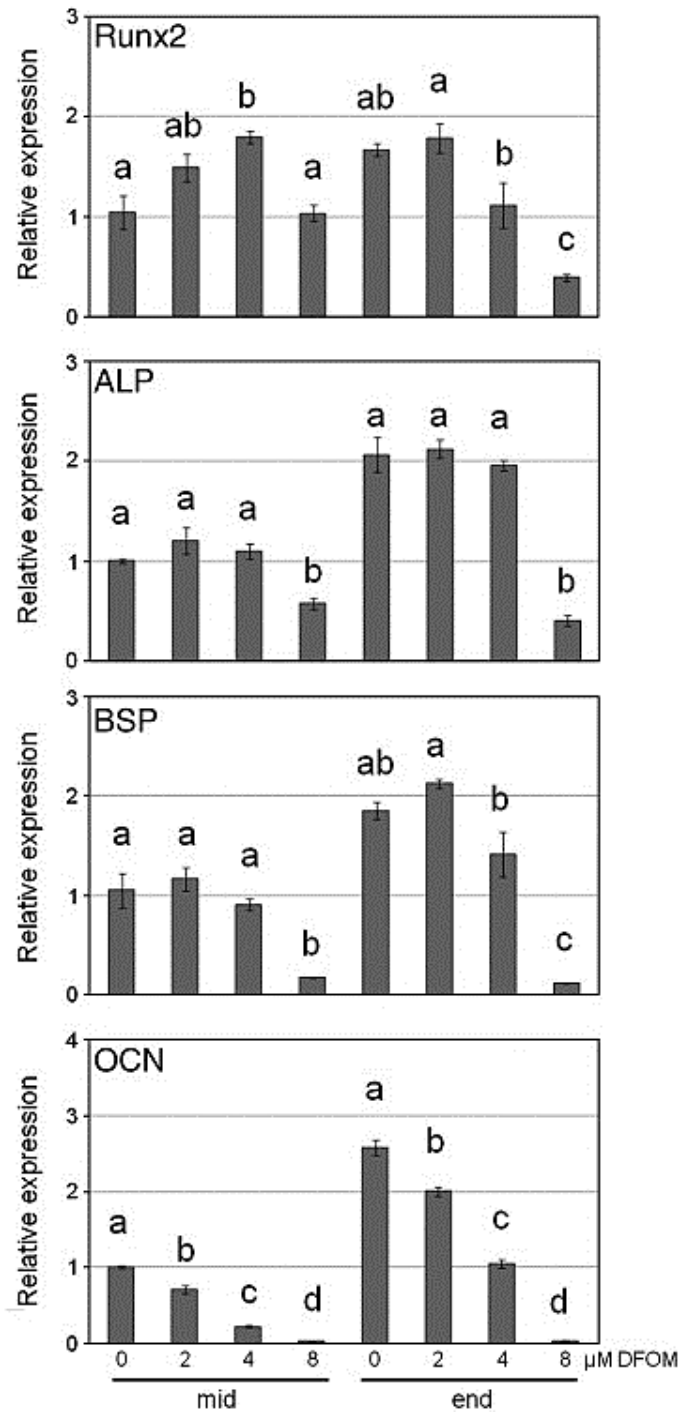


Fig. 4. Real-time PCR analysis of osteoblast phenotype genes and transcription factor Runx2 from cultures isolated from fetal rat calvaria and treated with 0-8 μ M DFOM throughout differentiation. Mid and end represent samples taken at midpoint (\sim D15) and end of differentiation (D21), respectively. L32 was the endogenous control and mid 0 μ M was used as calibrator sample. Data represent mean \pm SEM of 4 determinations. ANOVA: $p < 0.05$ with respect to day. Treatments that are significantly different ($p < 0.05$) as determined by Tukey post hoc analysis are assigned different letters. Treatments that are not significantly different ($p > 0.05$) are assigned the same letters. Similar results were observed in at least 2 independent studies.

Iron-regulated genes and proteins, but not osteoblast phenotype parameters return to control levels after 8 μ M DFOM treatment during early differentiation only

Real-time PCR of TrfR gene expression revealed that treatment with 8 μ M DFOM during early differentiation resulted in levels similar to control on D21, while treatment during late differentiation and continuous exposure to 8 μ M DFOM resulted in up-regulation of TrfR (Fig. 5A). TrfR protein expression exhibited a trend that was generally congruent with genes (Fig. 5B). PCR analysis of ferritin genes revealed no marked alterations after DFOM treatment at any time point (Fig. 5C). In contrast, continuous treatment or treatment only during late differentiation resulted in down-regulation of proteins, while treating cells during early differentiation resulted in ferritin protein expression similar to control (Fig. 5D).

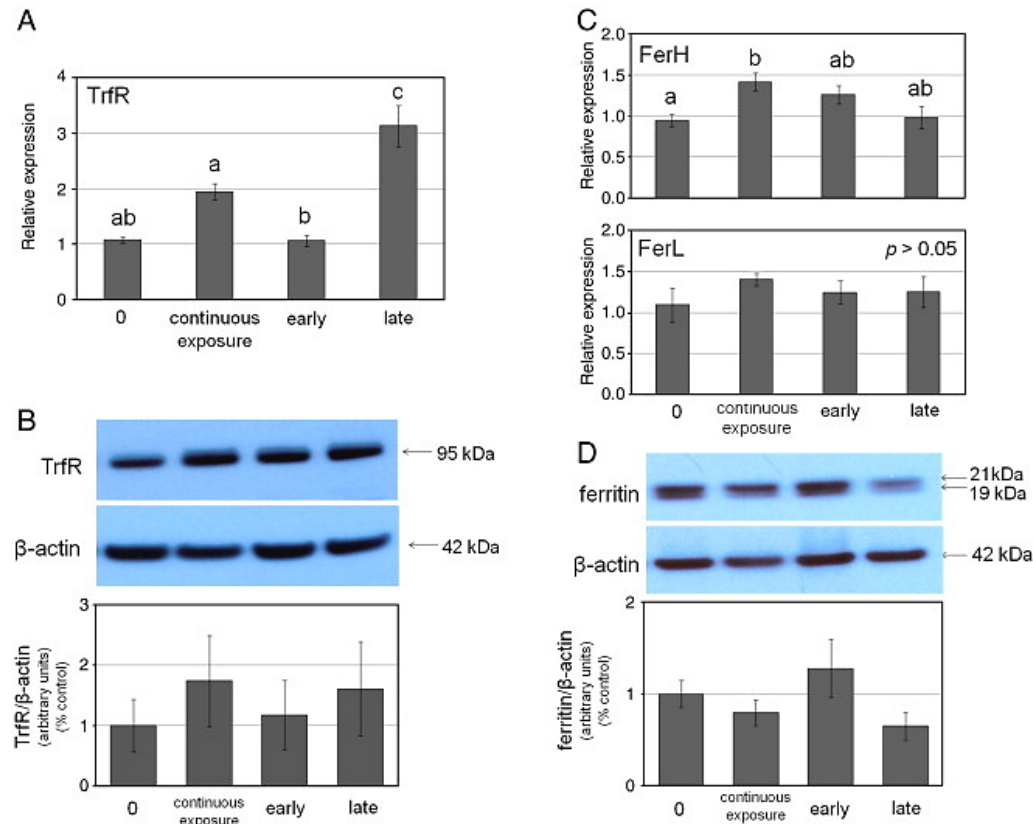


Fig. 5. Iron-regulated genes and proteins in fetal rat calvaria cultures on D21 treated with 8 μ M DFOM continuously or during early or late differentiation only. (A) Real-time PCR amplification of TrfR with L32 as endogenous control and 0 μ M as calibrator sample. (B) Western blots of TrfR and loading control β -actin. Semi-quantitative net intensity values normalized to β -actin and expressed as percent control (0 μ M). (C) Real-time PCR amplification of FerL and FerH with L32 as endogenous control and 0 μ M as calibrator sample. (D) Western blots of ferritin and loading control β -actin. Semi-quantitative net intensity values normalized to β -actin and expressed as percent control (0 μ M). Real-time PCR and Western blot data represent mean \pm SEM of 4 determinations. For PCR, ANOVA: $p < 0.05$ for all genes, except FerL. Treatments that are significantly different ($p < 0.05$) as determined by Tukey post hoc analysis are assigned different letters. Treatments that are not significantly different ($p > 0.05$) are assigned the same letters. Similar results were observed in 2 independent studies.

Representative wells of alkaline phosphatase and von Kossa stained osteoblast-like colonies in cultures treated with 8 μ M DFOM continuously or during early or late differentiation only are shown in Fig. 6A. Alkaline phosphatase staining was less intense after continuous treatment with 8 μ M DFOM and the percent of mineralized surface area was significantly lower after both continuous and early treatment with 8 μ M DFOM, a 72% ($p < 0.05$) and 40% ($p < 0.05$) decrease, respectively (Fig. 6B). The percent mineralized surface area after late treatment was about 20% lower and was not significantly different from control ($p > 0.05$). Microscopic evaluation revealed that the total number of nodules was 70% lower ($p < 0.05$) and the number of mineralized nodules was 80% lower ($p < 0.05$) in wells treated continuously with 8 μ M DFOM compared to controls (data not shown). Treatment during early or late differentiation resulted in about 30% lower mineralized nodules and total nodules per well for both groups, compared to control ($p > 0.05$, data not shown). The number of unmineralized nodules was similar among all groups ($p > 0.05$, data not shown).

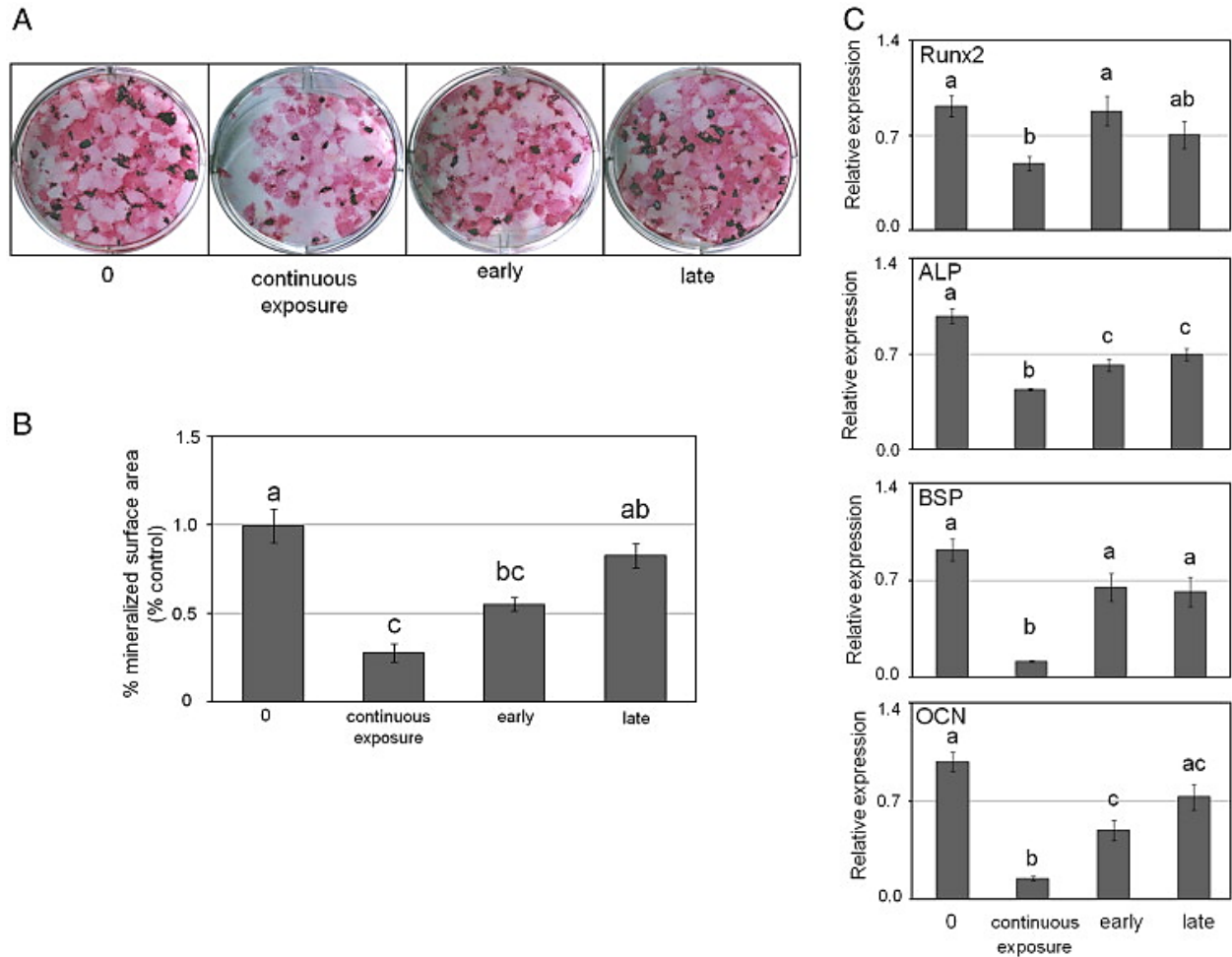


Fig. 6. Osteoblast-like colonies and osteoblast phenotype genes from fetal rat calvaria cultures on D21 treated with 8 μ M DFOM continuously or during early or late differentiation only. (A) Representative wells of alkaline phosphatase-positive colonies (pink) and mineralized bone nodules (black) on D21. (B) Average percent mineralized surface area expressed as a percent of control (0 μ M). Data represent mean \pm SEM of triplicate wells. (C) Real-time PCR of osteoblast phenotype genes and transcription factor Runx2 with L32 as endogenous control and 0 μ M as calibrator sample. Data represent mean \pm SEM of four determinations. ANOVA: $p < 0.05$ for genes and percent mineralized surface area; treatments that are significantly different ($p < 0.05$) as determined by Tukey post hoc analysis are assigned different letters. Treatments that are not significantly different ($p > 0.05$) are assigned the same letters. Similar results were seen in at least 2 independent studies.

Treating cells continuously during differentiation suppressed Runx2, ALP, BSP, and OCN at D21 compared to control (Fig. 6C). Treatment during early differentiation resulted in significant suppression of OCN and ALP ($p < 0.05$), but not Runx2 and BSP ($p > 0.05$) and a similar pattern of gene expression was seen after treatment during late differentiation only.

Discussion

These results demonstrate that chronic exposure of primary rat calvaria-derived osteoblasts to DFOM during differentiation suppresses osteoblast phenotypic development. Data also provide evidence that iron may be most critical during early differentiation. This study supports the hypothesis that iron deficiency-induced bone loss is the result of adverse effects on osteoblastogenesis.

In the classical model of iron-mediated regulation of cellular iron status, low levels of intracellular iron typically prevent TrfR mRNA degradation while blocking ferritin translation in an attempt to increase intracellular iron concentration. In the current study, the cells responded to DFOM by up-regulating TrfR gene and protein expression, while simultaneously down-regulating ferritin at the post-transcriptional level, suggesting that DFOM treatment lowered levels of intracellular iron. Furthermore, upon removal of DFOM, iron metabolism genes and proteins were restored to levels similar to control, suggesting dynamic alteration of iron-regulatory genes and proteins that reflect changes in iron availability. Together, these data suggest that iron regulation in osteoblasts follows classic intracellular iron-mediated regulation. This hypothesis is further supported by previous studies in fetal rat calvaria cultures in which iron-regulated genes and proteins have been shown to be responsive to changes in increased iron concentrations [20]. However, iron metabolism in osteoblasts remains poorly understood and tissue-specific mechanisms may exist that utilize a combination of transcriptional and post-translational modifications that ultimately determine final expression of iron uptake and storage proteins [21]. Also, ferritin expression in this culture system may not necessarily reflect an *in vivo* response to iron deficiency, since ascorbic acid, which is known to modulate ferritin metabolism [22], was present throughout the cell culture since it is required for the formation of nodules in fetal rat calvaria.

In fetal rat calvaria cultures, nodules containing mature osteoblasts that express osteocalcin are thought to emerge from committed osteoprogenitors in a linear progression [15]. DFOM treatment appears to interrupt one or more pathways vital to this progression, but whether this results in a delay of differentiation or irreversible suppression is unknown. DFOM dose-dependently down-regulated osteoblast gene markers after about one week of treatment. Similarly, DFOM resulted in suppression of mineralization, but in lower doses (2 and 4 μM), this suppression was mitigated so that percent mineralization resembled control at D21. Given the concomitant alterations in iron-regulatory genes and proteins, it appears that in standard differentiation media supplemented with low doses of DFOM, cells may compensate for decreased iron availability by altering expression of iron-metabolic proteins which results in outcomes that are favorable for supporting osteogenesis.

In contrast, chronic exposure to 8 μM DFOM produced marked and sustained suppression of osteoblast phenotype genes and Runx2, alkaline phosphatase-positive colonies and percent mineralized surface area, as well as lower total number of nodules. Taken together, these data

suggest that low iron availability may diminish osteoblastic phenotype in fetal rat calvaria by suppressing recruitment of cells into the osteoblast lineage. Additionally, prolonged DFOM exposure results in mineralized nodules that are markedly smaller than control, suggesting that the function of the recruited osteoblast-like cells in these colonies is also diminished. This sustained suppression of osteoblast phenotype and disrupted function occurred even though iron-regulatory mechanisms attempted to compensate for the presence of the iron chelator, providing evidence that progression of osteoblast differentiation requires a critical concentration of iron.

It appears that early differentiation events that are vital to progression from osteoprogenitor to osteoblast may be more dependent on iron availability than later events, and the suppression of phenotype after continuous treatment may be the result of sustained blockage of one or more early differentiation pathways. The suppression of osteoblast phenotype after treatment during early differentiation only was less severe than continuous treatment, suggesting that replenishment of iron to the media facilitates progression of differentiation that would otherwise be inhibited by continued exposure to 8 μ M DFOM. The recovery of the cells lends credence to the hypothesis that iron-deficient conditions may induce a delay in osteoblast progression, however, it is not known whether extending the culture period past D21 would have resulted in complete recovery of osteoblast phenotype.

Low intracellular iron is known to arrest the cell cycle, and in many cancer cells this is often followed by up-regulation of apoptotic processes [23]. In the osteoblastic MG-63 cell line, decreased proliferation has been reported after 48 h of treatment with DFOM in excess of 10 μ M [11]. In fetal rat calvaria, the primary proliferative phase occurs directly after plating and continues until confluence. This phase is reflected by high levels of DNA synthesis and cell cycle gene expression which fall to less than 20% of peak expression at confluence [14] and [24]. In the present study, all DFOM was administered after confluence, when differentiation is primarily characterized by matrix development, maturation, and mineralization [15]. Nonetheless, low levels of DNA synthesis have been shown to persist into early phases of differentiation when nascent nodules are multi-layering before gradually tapering off to negligible levels as differentiation progresses [24] and [25]. Therefore, the administration of DFOM may have had a suppressive effect on multi-layering potentially followed by promotion of pro-apoptotic pathways, which contributed to diminished osteoblastogenesis. Disrupted proliferation may also be a factor in the sustained suppression of osteoblast parameters observed after DFOM treatment during early differentiation rather than late differentiation, since later cultures would contain more post-mitotic osteoblasts. It should be noted that multi-layering occurs in concert with various external cues and intracellular signaling pathways, none of which are thought to be mutually exclusive, and are required for differentiation [14], [15] and [24]. This suggests that several mechanisms may contribute to iron deficiency's overall detrimental effects on osteoblast phenotype development during early differentiation.

The accumulation of extracellular collagen matrix during early phases of fetal rat calvaria culture also contributes to the progression of osteoblast differentiation and mineralization [24] and [26].

Moreover, the extensive post-translational modification required to form mature type I collagen fibrils involves two iron-requiring enzymes, prolyl and lysyl hydroxylase [27]. Thus, low intracellular iron availability during early differentiation may result in production of immature collagen fibrils which cannot support osteoblast phenotype development and are not competent for mineralization. Parelman et al [13] reported no difference in type I collagen protein levels in hFOB 1.19 cells treated with 8 μ M DFOM for 48 h compared to controls, but did not examine collagen maturation.

Existing studies in multiple cell types have consistently shown that the effects of DFOM are reversed by simultaneously incubating cells with DFOM and an equimolar concentration of iron salts [e.g. [11], [28],[29] and [30]]. These studies, when taken alongside the iron-metabolic gene and protein data in the present study, suggest that incubating cells with DFOM results in outcomes that are specific to iron availability.

These findings support existing evidence that iron deficiency produces bone loss via decreased osteoblastogenesis and provide insight into the mechanisms by which low iron may exert its effects. Although it appears that osteoblast differentiation may resume after iron is restored to adequate levels, even a transient interruption of bone formation may have long-term consequences *in vivo*, particularly since the two populations most vulnerable to iron deficiency anemia are children, who are still accruing bone mass, and women who will likely experience post-menopausal bone loss later in life. This study not only demonstrates an important role for iron in bone development, but underscores the need to develop effective prevention of iron deficiency anemia.

Conflict of interest

The authors have no conflicts of interest.

Acknowledgments

This work was supported in part through funds from the U.S. Department of Agriculture, Agricultural Research Service.

References

- [1] Handelman GJ, Levin NW. Iron and anemia in human biology: a review of mechanisms. *Heart Fail Rev* 2008;13:393–404.
- [2] World Health Organization. <http://www.who.int/nutrition/topics/ida/en/index.html> (accessed 26 June 2009).
- [3] Beard JL. Iron biology in immune function, muscle metabolism, and neuronal functioning. *J Nutr* 2001;131:568S–80S.

- [4] Harris MM, Houtkooper LB, Stanford VA, Parkhill C, Weber JL, Flint-Wagner H, et al. Dietary iron is associated with bone mineral density in healthy postmenopausal women. *J Nutr* 2003;133:3598–602.
- [5] Abraham R, Walton J, Russell L, Wolman R, Wardley-Smith B, Green JR, et al. Dietary determinants of post-menopausal bone loss at the lumbar spine: a possible beneficial effect of iron. *Osteoporos Int* 2006;17:1165–73.
- [6] Maurer J, Harris MM, Stanford VA, Lohman TG, Cussler E, Going SB, et al. Dietary iron positively influences bone mineral density in postmenopausal women on hormone replacement therapy. *J Nutr* 2005;135:863–9.
- [7] Medeiros DM, Plattner A, Jennings D, Stoecker B. Bone morphology, strength and density are compromised in iron-deficient rats and exacerbated by calcium restriction. *J Nutr* 2002;132:3135–41.
- [8] Medeiros DM, Stoecker B, Plattner A, Jennings D, Haub M. Iron deficiency negatively affects vertebrae and femurs in rats independently of energy intake and body weight. *J Nutr* 2004;134:3061–7.
- [9] Katsumata S-I, Tsuboi R, Uehara M, Suzuki K. Dietary iron deficiency decreases serum osteocalcin concentration and bone mineral density in rats. *Biosci Biotechnol Biochem* 2006;70(10):2547–50.
- [10] Katsumata S-I, Tsuboi R, Uehara M, Suzuki K. Severe iron deficiency decreases both bone formation and bone resorption in rats. *J Nutr* 2009;139:238–43.
- [11] Naves Díaz ML, Elorriaga R, Canteros A, Cannata Andía JB. Effect of desferrioxamine and deferiprone (L1) on the proliferation of MG-63 bone cells and on phosphatase alkaline activity. *Nephrol Dial Transplant* 1998;13(Suppl 3):23–8.
- [12] Malaval L, Modrowski D, Gupta AK, Aubin JE. Cellular expression of bone-related proteins during in vitro osteogenesis in rat bone marrow stromal cell cultures. *J Cell Physiol* 1994;158:555–72.
- [13] Parelman M, Stoecker B, Baker A, Medeiros D. Iron restriction negatively affects bone in female rats and mineralization of hFOB osteoblast cells. *Exp Biol Med (Maywood)* 2006;213:378–86.
- [14] Lian JB, Stein GS. Development of the osteoblast phenotype:molecular mechanisms mediating osteoblast growth and differentiation. *Iowa Orthop J* 1995;15:118–40.
- [15] Aubin JE. Advances in the osteoblast lineage. *Biochem Cell Biol* 1998;76(6): 899–910.

- [16] Kicic A, Chua ACG, Baker E. Effect of iron chelators on proliferation and iron uptake in hepatoma cells. *Cancer* 2001;92:3093–110.
- [17] Bridges KR, Cudkowicz A. Effect of iron chelators on transferrin receptor in K562 cells. *JBC* 1984;21(10):12970–7.
- [18] Bellows CG, Aubin JE, Heersche JNM, Antosz ME. Mineralized bone nodules formed in vitro from enzymatically released rat calvaria cell populations. *Calcif Tissue Int* 1986;38:143–54.
- [19] Bonnelye E, Chabadel A, Saltel F, Jurdic P. Dual effect of strontium ranelate: stimulation of osteoblast differentiation and inhibition of osteoclast formation and resorption in vitro. *Bone* 2008;42(1):129–38.
- [20] Messer JG, Kilbarger AK, Erikson KM, Kipp DE. Iron overload alters iron-regulatory genes and proteins, down-regulates osteoblastic phenotype, and is associated with apoptosis in fetal rat calvaria cultures. *Bone* 2009;45(5):972–9.
- [21] Eisenstein RS. Iron regulatory proteins and the molecular control of mammalian iron metabolism. *Annu Rev Nutr* 2000;20:627–62.
- [22] Toth I, Bridges KR. Ascorbic acid enhances ferritin mRNA translation by an IRP/aconitase switch. *J Biol Chem* 1995;270(33):19540–4.
- [23] Yu Y, Kovacevic Z, Richardson DR. Tuning cell cycle regulation with an iron key. *Cell Cycle* 2007;6(16):1982–94.
- [24] Owen TA, Aronow M, Shalhoub V, Barone LM, Wilming L, Tassinari MS, et al. Progressive development of the rat osteoblast phenotype in vitro: reciprocal relationships in expression of genes associated with osteoblast proliferation and differentiation during formation of the bone extracellular matrix. *J Cell Physiol* 1990;143:420–30.
- [25] Lynch MP, Capparelli C, Stein JL, Stein GS, Lian JB. Apoptosis during bone-like tissue development in vitro. *J Cell Biochem* 1998;68(1):31–49.
- [26] Lynch MP, Stein JL, Stein GS, Lian JB. The influence of type I collagen on the development and maintenance of the osteoblast phenotype in primary and passaged rat calvarial osteoblasts: modification of expression of genes supporting cell growth, adhesion, and extracellular matrix mineralization. *Exp Cell Res* 1995;216:35–45.
- [27] Bornstein P. The biosynthesis of collagen. *Annu Rev Biochem* 1974;43:567–603.
- [28] Alcantara O, Boldt DH. Iron deprivation blocks multilineage haematopoietic differentiation by inhibiting induction of p21(WAF1/CIP1). *Br J Haematol* 2007;137: 252–61.

[29] Morath DJ, Mayer-Pröschel M. Ironmodulates the differentiation of a distinct population of glial precursor cells into oligodendrocytes. *Dev Biol* 2001;237:232–43.

[30] Brard L, Granai CO, Swamy N. Iron chelators deferoxamine and diethylenetriamine pentaacetic acid induce apoptosis in ovarian carcinoma. *Gynecol Oncol* 2006;100: 116–27.